Journal of Solid Mechanics Vol. 11, No. 1 (2019) pp. 222-235
DOI: 10.22034/JSM.2019.664231

Nonlinear Modeling of Bolted Lap Jointed Structure with Large Amplitude Vibration of Timoshenko Beams

M. Jamal-Omidi *, F. Adel

Department of Aerospace Engineering, Space Research Institute, Malek Ashtar University of Technology, Tehran, Iran

Received 10 January 2019; accepted 8 March 2019

ABSTRACT

This paper aims at investigating the nonlinear behavior of a system which is consisting of two free-free beams which are connected by a nonlinear joint. The nonlinear system is modelled as an in-extensional beam with Timoshenko beam theory. In addition, large amplitude vibration assumption is taken into account in order to obtain exact results. The nonlinear assumption in the system necessities existence of the curvature-related and inertia-related nonlinearities. The nonlinear partial differential equations of motion for the longitudinal, transverse, and rotation are derived using the Hamilton's principle. A set of coupled nonlinear ordinary differential equations are further obtained with the aid of Galerkin method. The frequency-response curves are presented in the section of numerical results to demonstrate the effect of the different dimensionless parameters. It is shown that the nonlinear bolted-lap joint structure exhibits a hardening-type behavior. Furthermore, it is found that by adding a nonlinear spring the system exhibits a stronger hardening-type behavior. In addition, it is found that the system shows nonlinear behavior even in the absence of the nonlinear spring due to the nonlocal nonlinearity assumption. Moreover, it is shown that considering different engineering beam theories lead to different results and it is found that the Euler-Bernoulli beam theory over-predict the resonance frequency of the structure by ignoring rotary inertia and shear deformation.

Keywords : Bolted lap joint structure; Local nonlinearity; Nonlocal nonlinearity; Timoshenko beam theory; Nonlinear vibration.

1 INTRODUCTION

DYNAMIC characteristics of a structure with mechanical joints certainly depend on the dynamic characteristics of the joints. Thus, the dynamic characteristics of the joints should be identified accurately before conducting the vibration analysis for the structure [1]. In recent years, the lack of a complete research work in the literature on the mechanical response of the bolted lap joint structures have motivated investigator on the subject [2, 3]. Ahmadian and Jalali [4] both experimentally and analytically have identified the parameters of bolted joints in assembled structures. The authors used the first three natural frequencies to identify the linear lateral stiffness and

*Corresponding author. Tel.: +98 21 44251196; Fax: +98 21 44251196.
E-mail address: j_omidi@mut.ac.ir (M. Jamal-Omidi).

torsional stiffness of assembled structure. Ma et al. [5] performed a similar experiment and studied the effect of the joints in dynamics of beam structure. The authors detected three levels of joint tightening by investigating the nonlinear and loosing effect which comes from damping of joint. The authors concluded that their method can be used to every bolted structure with the aim of identifying the system parameters. Jalali et al. [6] represented the bolted lap joint with a damper which has linear viscous and cubic stiffness. The authors by employing steady state response of the structure and force state mapping technique identified joint parameters for different excitation levels. Based on the literature there are two kinds of modeling methods for joints: non-linear joint models [7-17] and linear joint models [18-21]. Generally, considering friction related nonlinearities in the interface surfaces necessitates using nonlinear joint models. Because a frictional joint owns complex mechanism (macro-slip and micro-slip behavior), deep understanding and analytical descriptions of the joints and interface is a mandatory for the nonlinear models [22]. From researchers' perspective, nonlinear joints modeling applicability in experimental researches and their validity in practical applications are not completely satisfactory [23]. Liao and Zhang [7] built a non-linear damping model of bolted-joint interface by considering viscous damping and coulomb friction. The authors conducted vibration experiments with different bolted preloads. Their results illustrated that in lower excitation levels the most interface of bolted joint occurs stick-slip motions. Chatterjee and Vyas [8] presented an approach of identification of parametric system in their study. The authors have carried out a numerical simulation for a typical Duffing oscillator and investigated robustness of the estimation procedure in the presence of measurement noise. Later, the same authors Chatterjee and Vyas [9] have developed a structured response representation of various harmonics under multi-input harmonic excitations by employing multi-input Volterra series. In their modeling the nonlinearity has considered in the form of polynomial with general square and cubic terms. The authors observed that a high accuracy in their estimation due to the existence of the higher order component in harmonic amplitude. Kerschen et al. [10] have published an overview paper with focusing on structural system identification in the presence of nonlinearity. Thothadri et al. [11] studied a MDOF system with purpose of identification of the nonlinear systems parameters by using theoretical approaches namely, harmonic balance and bifurcation methods. The authors observed that using methodology of bifurcation theory system identification excellently capture the stable and unstable limit cycles within the experimental regime. Thothadri et al. [12] used the same approach, harmonic balance method, for the nonlinear system. The authors found that if the model structure is well known, their methodology performs well in capturing the unknown parameters. And also they found that if the model is not well known, the methodology is able to capture the stable limit cycle but not the unstable limit cycle. Hajj et al. [13] have combined perturbation technique and spectral moments to characterize and quantify the damping and nonlinear parameters of the first mode of a three-beams and two-frames, which frame is harmonically excited near to twice its lowest natural frequency. They determined the damping and nonlinear parameters of their structure by using amplitude and phase difference between the excitation and response mode with different frequencies. Noël et al. [14] have presented a comprehensive review on the parameter identification of the nonlinear structural dynamics. Maio [15] both experimentally and numerically investigated the identification of the nonlinear behavior of bolted structures. The author developed correlation methods by using experimental tests and parameters. Ahmadian et al. [16] studied the stability of a beam subjected to thrust which acts as a follower non-conservative force. Their system includes two interconnected beams with a nonlinear joint. Authors have obtained the flutter and divergence and post-critical behaviors in their considered system.

It is worthy to mention that the importance of joint nonlinear influence to the dynamic behavior of structures could be changed from case to case. For instance, for the low levels of excitation, a friction joint can behave such a linear component [24]. On the other hand of what have presented a short review on the nonlinear modeling of joints above, linear modeling which consists of constant mass, stiffness and damping properties which are considered as firm fastened connection are introduced. In addition, the influence of the substrates on the dynamic behavior of structures is very important and should be taken into account. The nonlinear dynamics behavior of nonlocal Timoshenko beam theory has widely studied by Ghorbanpour Arani et al. [25-27].

Based on the literature, most of researchers have been mostly focused on the localized nonlinearities induced by a nonlinear spring derived from nonlinear joint modeling. The present study focus on the obtaining stable and unstable bifurcation points of a nonlinear system with the presence of the local and nonlocal nonlinearities simultaneously. In addition, in the past works most of the researchers are simplified the transverse vibration of the substructures by employing Euler-Bernoulli model assumption. Which this theory ignores the influence of the shear deformation and rotary inertia. Therefore, we have taken into account the effect of these parameters on the nonlinear joint structures behavior, and the substructures are modelled by the Timoshenko model. Accordingly, it seems that studying two bolted free-free beams by using Timoshenko beam theory by considering large amplitude vibration and nonlinear springs and a torsional damper located in the joint interface of the beams, gives interesting results. The numerical results are presented in the form of frequency-response curves to demonstrate the effect of the different

parameters. It is shown that in the presence and in the increasing value of the linear spring and absence of the nonlinear spring, natural frequency is occurred at higher frequency and the corresponding maximum amplitude is decreased. Numerically, it is shown that increasing in values of the linear damping coefficient and forcing amplitude resulted in decreasing and increasing in maximum amplitude of the system, respectively.

2 MATHEMATICAL FORMULATIONS

Fig. 1 shows the considered bolted lap joint structure that consists of two free-free beams and an attached tip mass at free ends of one of the beams. In order to model the bolted joint interface, a combination of the linear spring, linear and nonlinear torsional spring, and linear torsional damping are used. The beams of length L_{bi}, thickness t_{bi}, and widthw_{bi}; where i indicates the number of the beams. A block tip mass, M_t is of length and height of h_1 and h_2, respectively. It is assumed that one single harmonic base excitation in the form of $F(t)=F_0\sin(\omega t)$, with F_0 being excitation amplitude and ω is the frequency amplitude. In addition, $w_i(x,t)$, $u_i(x,t)$, and $\phi(x,t)$ are used in order to denote the transverse, axial and rotation displacements as shown in figure. Also, uniform mass distribution assumption is considered in order to avoid the complexity in the theoretical procedure in this paper.

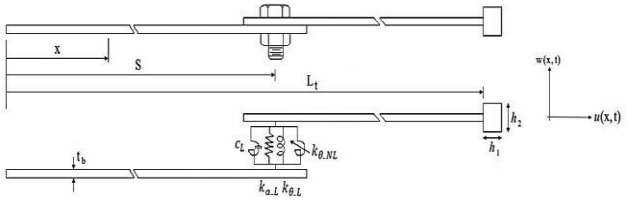

Fig.1
A schematic of the free-free assembled beam with nonlinear joint and nonlinear substructures.

The total kinetic energy of the system is composed of the kinetic energies of the free-free beams, and the tip mass. The kinetic energy of the free-free beams can be written as follows [28]:

$$T_{b1}=\frac{1}{2}\rho A\int_o^L\left[\left(\frac{\partial u_1}{\partial t}\right)^2+\left(\frac{\partial w_1}{\partial t}\right)^2\right]dx+\frac{1}{2}\rho I\int_o^L\left(\frac{\partial \phi_1}{\partial t}\right)^2dx \tag{1}$$

$$T_{b2}=\frac{1}{2}\rho A\int_L^{2L}\left[\left(\frac{\partial u_2}{\partial t}\right)^2+\left(\frac{\partial w_2}{\partial t}\right)^2\right]dx+\frac{1}{2}\rho I\int_L^{2L}\left(\frac{\partial \phi_2}{\partial t}\right)^2dx \tag{2}$$

where A, ρ and I are cross sectional, the mass density and area moment of inertia of the beams, respectively. The vector $\vec{r}_M$ as a distance of the base of the beam to the center of the tip mass is defined in order to formulate the kinetic energy of the block mass :

$$\vec{r}_M=\left(L_t+\frac{h_1}{2}\cos\psi(L_t,t)\right)\vec{e}_1+\left(w(L_t,t)+\frac{h_1}{2}\sin\psi(L_t,t)\right)\vec{e}_2 \tag{3}$$

where $\psi(x,t)$ is the slope of the beam with respect to the horizontal axis (see Ref. [29]). $\vec{e}_1$, $\vec{e}_2$ and L_t are unit axial vectors in the u and v directions, and whole length of the system, respectively. Accordingly, time derivative of the position vector $\vec{r}_M$, is given by [30]:

$$\dot{\vec{r}}_M=\left(-\frac{a}{2}\dot{\psi}(L_t,t)w'\right)\vec{e}_1+\left(\dot{w}(L_t,t)+\frac{a}{2}\dot{\psi}(L_t,t)\right)\vec{e}_2 \tag{4}$$

The tip mass kinetic energy's is defined as follows:

$$T_M = \frac{1}{2} M_t \dot{\vec{r}}_M \cdot \dot{\vec{r}}_M + \frac{1}{2} I_M \dot{\psi}^2 (L_t, t) \tag{5}$$

where I_M is the moment of inertia of the tip mass about its center of gravity. The total kinetic energy of the bolted lap joint structure can be found by summing the Eqs. (1), (2), and (5).

The variation of the work done by the external forces, which is generally comprised of the harmonic excitation force and the viscose damping force due to the surrounding medium, are expressed as [31]:

$$\delta W_F = \int_0^L b_0 \cos(\omega t) \delta w_1 dx \tag{6}$$

$$\begin{aligned} \delta W_D = & -c_d \int_0^L \left(\frac{\partial u_1}{\partial t} \delta u_1 + \frac{\partial w_1}{\partial t} \delta w_1 \right) dx - c_r \int_0^L \left(\frac{\partial \phi_1}{\partial t} \delta \phi_1 \right) dx - c_d \int_L^{2L} \left(\frac{\partial u_2}{\partial t} \delta u_2 + \frac{\partial w_2}{\partial t} \delta w_2 \right) dx - c_r \int_L^{2L} \left(\frac{\partial \phi_2}{\partial t} \delta \phi_2 \right) dx \\ & - c \left(\frac{\partial^2 w_2}{\partial t \partial x} - \frac{\partial^2 w_1}{\partial t \partial x} \right) (\delta w_2 - \delta w_1) \end{aligned} \tag{7}$$

where c_d and c_r are the viscos damping coefficients for the displacements and rotation coordinates, respectively. And c is the damping coefficient from the bolted lap joint structure modelling.

The total potential energy of the system which is consists of potential energy of each beam, linear and nonlinear transverse and torsional springs, and is written as following:

$$U_T = U_{b1} + U_{b2} + U_{LS} + U_{NTS} \tag{8}$$

where U_{b1} and U_{b2} are potential energies of the beam #1 and #2 respectively, and U_{LS} and U_{NTS} are potential energies of the linear spring and linear and nonlinear torsional springs respectively. In what follows, the equation of each potential energy is obtained. Any axial displacement which can be caused by shear deformation are neglected in current research, in the Timoshenko beam theory are given by [28]:

$$w = w_s + w_b, \quad \beta = \frac{\partial w_s}{\partial x} \tag{9a}$$

$$u = -z \left(\frac{\partial w}{\partial x} - \beta \right) = -z \, \phi(x, t) \tag{9b}$$

$$v = 0, \quad w = w(x, t) \tag{9c}$$

where w is the total transverse displacement, w_s and w_b are shear and bending displacements, respectively, β is the shear deformation or shear angle, and v is lateral displacement. Where the strains corresponding to the displacement fields given by Eq. (9), and using Von-Karman strain Equation [32], one may obtain Eq. (10) as follows:

$$\varepsilon_{xx} = \frac{\partial u}{\partial x} + \frac{1}{2} \left[\left(\frac{\partial u}{\partial x} \right)^2 + \left(\frac{\partial w}{\partial x} \right)^2 \right] \tag{10a}$$

$$\varepsilon_{xx} = -z \frac{\partial \phi}{\partial x} + \frac{1}{2} \left[\left(\frac{\partial u}{\partial x} \right)^2 + \left(\frac{\partial w}{\partial x} \right)^2 \right] \tag{10b}$$

$$\varepsilon_{zx} = \frac{\partial u}{\partial x} + \frac{\partial w}{\partial x} = -\phi(x,t) + \frac{\partial w}{\partial x} \tag{10c}$$

which for the sake of completeness, the effect of the longitudinal displacement in the equation of motion of the system is taken into account. The components of stress corresponding to the strains of Eq. (10) are given by:

$$\sigma_{xx} = E\,\varepsilon_{xx} = -Ez\,\frac{\partial \phi}{\partial x} + \frac{1}{2}E\left[\left(\frac{\partial u}{\partial x}\right)^2 + \left(\frac{\partial w}{\partial x}\right)^2\right] \tag{11a}$$

$$\sigma_{xx} = k'G\left(\frac{\partial w}{\partial x} - \beta\right) \tag{11b}$$

where E_b, G and $k' = 10(1+\upsilon)/(12+11\upsilon)$ are Young's modulus, shear modulus, and shear factor for the rectangle cross section, respectively, where υ being Poisson ratio. The strain energy of the beam U_b occupying region V can be determined as:

$$U_b = \frac{1}{2}\iiint (\sigma_{xx}\varepsilon_{xx} + \sigma_{zx}\varepsilon_{zx})dV \tag{12}$$

By substituting Eqs. (10) and (11) into Eq. (12), one may obtain the Eq. (13) as follows:

$$U_b = \frac{1}{2}\int_0^L \left[E_b I_b\left(\frac{\partial \phi}{\partial x}\right)^2 + E_b A_b\left(\frac{\partial u}{\partial x} + \frac{1}{2}\left(\frac{\partial w}{\partial x}\right)^2\right)^2 + k'GA_b\left(\frac{\partial w}{\partial x} - \beta\right)^2\right]dx \tag{13}$$

where I_b and A_b are area moment of inertia and cross sectional area of the beams, respectively. The potential energies of the linear spring, and linear and nonlinear torsional springs can be written as follows:

$$U_{LS} = \frac{1}{2}k_1(w_2 - w_1)^2\,\delta(x - S) \tag{14}$$

$$U_{NTS} = \left[\frac{1}{2}k_\theta\left(\frac{\partial w_2(x,t)}{\partial x} - \frac{\partial w_1(x,t)}{\partial x}\right)^2 - \frac{1}{4}k_{\theta NL}\left(\frac{\partial w_2(x,t)}{\partial x} - \frac{\partial w_1(x,t)}{\partial x}\right)^4\right]\delta(x - S) \tag{15}$$

3 FULL NONLINEAR EQUATIONS OF MOTION AND THE METHOD OF SOLUTION

In what follows, following [31], the Hamilton's principle (Eq. (16)) is utilized to drive the nonlinear equation motion of the nonlinear system [33]:

$$\delta\int_{t_1}^{t_2}\left[T(t) - U(t)\right]dt + \int_{t_1}^{t_2}\left[\delta W_F + \delta W_D + \delta W_p\right]dt = 0 \tag{16}$$

where δ denotes variational operator. Substituting, Eqs. (4) -(7) and (13) -(15) into the Hamilton's principle which is given by Eq. (16) yields the following nonlinear electromechanical partial differential equations of motion governing the longitudinal, transverse, rotational motions, of the nonlinear structure as follows:

$$\rho A\,\frac{\partial^2 u_1}{\partial t^2} - EA\left[\frac{\partial^2 u_1}{\partial x^2} + \frac{\partial w_1}{\partial x}\frac{\partial^2 w_1}{\partial x^2}\right] + c_d\,\frac{\partial u_1}{\partial t} = 0 \tag{17}$$

$$\rho A\frac{\partial^2 w_1}{\partial t^2}-EA\left[\frac{\partial^2 u_1}{\partial x^2}\frac{\partial w_1}{\partial x}+\frac{\partial u_1}{\partial x}\frac{\partial^2 w_1}{\partial x^2}+\frac{3}{2}\left(\frac{\partial w_1}{\partial x}\right)^2\left(\frac{\partial^2 w_1}{\partial x^2}\right)\right]-k'GA\left[\frac{\partial^2 w_1}{\partial x^2}-\frac{\partial \phi_1}{\partial x}\right]$$
$$+\left[-c\left(\frac{\partial^2 w_2}{\partial t\,\partial x}-\frac{\partial^2 w_1}{\partial t\,\partial x}\right)+k_1(w_2-w_1)+k_\theta\left(\frac{\partial w_2(x,t)}{\partial x}-\frac{\partial w_1(x,t)}{\partial x}\right)\right. \tag{18}$$
$$\left.-3k_{\theta NL}\left(\frac{\partial w_2(x,t)}{\partial x}-\frac{\partial w_1(x,t)}{\partial x}\right)^2\left(\frac{\partial^2 w_2(x,t)}{\partial x^2}-\frac{\partial^2 w_1(x,t)}{\partial x^2}\right)\right]\delta(x-S)+c_d\frac{\partial w_1}{\partial t}-b_0\cos(\omega t)=0$$

$$\rho I\frac{\partial^2 \phi_1}{\partial t^2}-EI\frac{\partial^2 \phi_1}{\partial x^2}+k'GA\left[\frac{\partial w_1}{\partial x}-\phi_1\right]+c_r\frac{\partial \phi_1}{\partial t}=0 \tag{19}$$

$$\rho A\frac{\partial^2 u_2}{\partial t^2}-EA\left[\frac{\partial^2 u_2}{\partial x^2}+\frac{\partial w_2}{\partial x}\frac{\partial^2 w_2}{\partial x^2}\right]+c_d\frac{\partial u_2}{\partial t}=0 \tag{20}$$

$$(\rho A+M)\frac{\partial^2 w_2}{\partial t^2}-EA\left[\frac{\partial^2 u_2}{\partial x^2}\frac{\partial w_2}{\partial x}+\frac{\partial u_2}{\partial x}\frac{\partial^2 w_2}{\partial x^2}+\frac{3}{2}\left(\frac{\partial w_2}{\partial x}\right)^2\left(\frac{\partial^2 w_2}{\partial x^2}\right)\right]+k'GA\left[\frac{\partial^2 w_2}{\partial x^2}-\frac{\partial \phi_2}{\partial x}\right]$$
$$+\left[c\left(\frac{\partial^2 w_2}{\partial t\,\partial x}-\frac{\partial^2 w_1}{\partial t\,\partial x}\right)-k_1(w_2-w_1)-k_\theta\left(\frac{\partial w_2(x,t)}{\partial x}-\frac{\partial w_1(x,t)}{\partial x}\right)\right. \tag{21}$$
$$\left.+3k_3\left(\frac{\partial w_2(x,t)}{\partial x}-\frac{\partial w_1(x,t)}{\partial x}\right)^2\left(\frac{\partial^2 w_2(x,t)}{\partial x^2}-\frac{\partial^2 w_1(x,t)}{\partial x^2}\right)\right]\delta(x-S)+c_d\frac{\partial w_1}{\partial t}=0$$

$$\rho I\frac{\partial^2 \phi_2}{\partial t^2}-EI\frac{\partial^2 \phi_2}{\partial x^2}+k'GA\left[\frac{\partial w_2}{\partial x}-\phi_2\right]+c_r\frac{\partial \phi_2}{\partial t}=0 \tag{22}$$

where $M=M_t\left(A_1+\frac{h_1}{2}A_2\right)^2+I_M NA_2^2$. A_1 and A_2 are defined in Appendix.

The following dimensionless parameters in order to find the dimensionless nonlinear equations of motion are introduced:

$$x^*=\frac{x}{L},\quad u_1^*=\frac{u_1}{L},\quad w_1^*=\frac{w_1}{L},\quad \phi_1^*=\phi_1,\quad u_2^*=\frac{u_2}{L},\quad w_2^*=\frac{w_2}{L},\quad \phi_2^*=\phi^*,\quad S^*=\frac{S}{L},$$
$$t^*=t\sqrt{\frac{EI}{\rho AL^4}},\quad \Omega=\omega\sqrt{\frac{\rho AL^4}{EI}},\quad \beta=\sqrt{\frac{EAL^2}{EI}},\quad \alpha=\sqrt{\frac{k'GAL^2}{EI}},\quad \eta=\sqrt{\frac{k'GA^2L^4}{EI^2}},$$
$$c_d^*=\frac{c_dL^4}{EI}\sqrt{\frac{EI}{\rho AL^4}},\quad c_r^*=\frac{c_rAL^4}{EI^2}\sqrt{\frac{EI}{\rho AL^4}},\quad k_1^*=\frac{k_1L^4}{EI},\quad k_\theta^*=\frac{k_\theta L^2}{EI},\quad k_{\theta NL}^*=\frac{3k_{\theta NL}L^2}{EI}, \tag{23}$$
$$c^*=\frac{cL^3}{EI}\sqrt{\frac{EI}{\rho AL^4}},\quad b_0^*=\frac{b_0L^3}{EI}$$

Substituting parameters introduced in Eq. (23) into Eqs. (17)-(22), and dropping asterisk notation for briefness, the results in the following dimensionless nonlinear partial differential equation of motion for the longitudinal, transverse, rotation motions, and the electromechanical relation, respectively, are expressed as:

$$\frac{\partial^2 u_1}{\partial t^2}-\beta^2\left[\frac{\partial^2 u_1}{\partial x^2}+\frac{\partial w_1}{\partial x}\frac{\partial^2 w_1}{\partial x^2}\right]+c_d\frac{\partial u_1}{\partial t}=0 \tag{24}$$

$$\frac{\partial^2 w_1}{\partial t^2}-\beta^2\left[\frac{\partial^2 u_1}{\partial x^2}\frac{\partial w_1}{\partial x}+\frac{\partial u_1}{\partial x}\frac{\partial^2 w_1}{\partial x^2}+\frac{3}{2}\left(\frac{\partial w_1}{\partial x}\right)^2\left(\frac{\partial^2 w_1}{\partial x^2}\right)\right]-\alpha^2\left[\frac{\partial^2 w_1}{\partial x^2}-\frac{\partial \varphi_1}{\partial x}\right]$$
$$+\left[-c\left(\frac{\partial^2 w_2}{\partial t\,\partial x}-\frac{\partial^2 w_1}{\partial t\,\partial x}\right)+k_1(w_2-w_1)+k_\theta\left(\frac{\partial w_2(x,t)}{\partial x}-\frac{\partial w_1(x,t)}{\partial x}\right)\right. \tag{25}$$
$$\left.-k_{\theta NL}\left(\frac{\partial w_2(x,t)}{\partial x}-\frac{\partial w_1(x,t)}{\partial x}\right)^2\left(\frac{\partial^2 w_2(x,t)}{\partial x^2}-\frac{\partial^2 w_1(x,t)}{\partial x^2}\right)\right]\delta(x-S)+c_d\frac{\partial w_1}{\partial t}-b_0\cos(\omega t)=0$$

$$\frac{\partial^2 \phi_1}{\partial t^2}-\beta^2\frac{\partial^2 \phi_1}{\partial x^2}+\eta^2\left[\frac{\partial w_1}{\partial x}-\phi_1\right]+c_r\frac{\partial \phi_1}{\partial t}=0 \tag{26}$$

$$\frac{\partial^2 u_2}{\partial t^2}-\beta^2\left[\frac{\partial^2 u_2}{\partial x^2}+\frac{\partial w_2}{\partial x}\frac{\partial^2 w_2}{\partial x^2}\right]+c_d\frac{\partial u_2}{\partial t}=0 \tag{27}$$

$$\left(1+\frac{M}{\rho A}\right)\frac{\partial^2 w_2}{\partial t^2}-\beta^2\left[\frac{\partial^2 u_2}{\partial x^2}\frac{\partial w_2}{\partial x}+\frac{\partial u_2}{\partial x}\frac{\partial^2 w_2}{\partial x^2}+\frac{3}{2}\left(\frac{\partial w_2}{\partial x}\right)^2\left(\frac{\partial^2 w_2}{\partial x^2}\right)\right]-\alpha^2\left[\frac{\partial^2 w_2}{\partial x^2}-\frac{\partial \phi_2}{\partial x}\right]$$
$$+\left[c\left(\frac{\partial^2 w_2}{\partial t\,\partial x}-\frac{\partial^2 w_1}{\partial t\,\partial x}\right)-k_1(w_2-w_1)-k_\theta\left(\frac{\partial w_2(x,t)}{\partial x}-\frac{\partial w_1(x,t)}{\partial x}\right)\right. \tag{28}$$
$$\left.+3k_{\theta NL}\left(\frac{\partial w_2(x,t)}{\partial x}-\frac{\partial w_1(x,t)}{\partial x}\right)^2\left(\frac{\partial^2 w_2(x,t)}{\partial x^2}-\frac{\partial^2 w_1(x,t)}{\partial x^2}\right)\right]\delta(x-S)+c_d\frac{\partial w_1}{\partial t}=0$$

$$\frac{\partial^2 \phi_2}{\partial t^2}-\beta^2\frac{\partial^2 \phi_2}{\partial x^2}+\eta^2\left[\frac{\partial w_2}{\partial x}-\phi_2\right]+c_r\frac{\partial \phi_2}{\partial t}=0 \tag{29}$$

4 THE REDUCED ORDER MODEL BASED ON GALERKIN METHOD

To obtain the reduced order model of the partial equations of motion, Eqs. (24)-(29), the Galerkin discretized method is utilized, and the displacements of the system are assumed as the following approximate series expansion [31, 34]:

$$w(x,t)=\sum_{k=1}^{M}\varphi_k(x)q_k(t) \tag{30}$$

$$\phi(x,t)=\sum_{k=1}^{N}\psi_k(x)p_k(t) \tag{31}$$

$$u(x,t)=\sum_{k=1}^{Q}\varphi_k(x)r_k(t) \tag{32}$$

where $\varphi_k(x)$ and $\psi_k(x)$ are the k^{th} Eigen functions for the transverse and rotation vibrations of a linear and undamped cantilevered piezoelectric beam, as comparison functions, respectively, and $q_k(t)$, $p_k(t)$, and $r_k(t)$ are the associated time-varying generalized coordinates of transverse, longitudinal, and rotational motions, respectively. To obtain the Eigen functions for the transverse and rotation vibrations, one may apply the exact Timoshenko beam theory which are provided in Ref. [35]. In this study, according to Refs. [28, 31], for the transverse vibrations Eigen function, it is sufficient to use from Euler-Bernoulli beam theory for the clamped-free conditions, and for the

Timoshenko beam theory to satisfy the exact mode shape based on Rayleigh-Ritz method, one may use $\psi(x) = \partial\varphi / \partial x$, to obtain the rotation vibrations Eigen function. Hence, Eigen functions for the cantilevered beam are expressed as follows:

$$\varphi_k(x) = \cos(\lambda_k x) - \cosh(\lambda_k x) - \sigma_1 \left[\sin(\lambda_k x) - \sinh(\lambda_k x)\right] \tag{33}$$

$$\psi_k(x) = -\sin(\lambda_k x) - \sinh(\lambda_k x) - \sigma_1 \left[\cos(\lambda_k x) - \cosh(\lambda_k x)\right] \tag{34}$$

where σ_1 is given by:

$$\sigma_1 = \frac{\cos(\lambda_k x) + \cosh(\lambda_k x)}{\sin(\lambda_k x) - \sinh(\lambda_k x)} \tag{35}$$

where the eigenvalue λ_k are obtained by solving frequency equation of the cantilevered beam as follows:

$$1 + \cos(\lambda L) + \cosh(\lambda L) = 0 \tag{36}$$

In order to obtain a set of nonlinear ordinary differential equations of motion of the system, the Galerkin technique, Eqs. (30) -(32), are substituted into Eqs. (24) -(29), and the resultant equations are multiplied by the corresponding Eigen function and integrated with respect to *x* from 0 to 1, and considering the single mode vibration, one may obtain the following nonlinear ordinary differential equations:

$$\ddot{r}_{11} - \beta^2 \left[\frac{N_2}{N_1} r_{11} + \frac{N_3}{N_1} {q_{11}}^2\right] + c_d \dot{r}_{11} = 0 \tag{37}$$

$$\begin{aligned} &\ddot{q}_{11} - \beta^2 \left[2\frac{N_3}{N_1} r_{11} q_{11} + \frac{3}{2}\frac{N_4}{N_1} {q_{11}}^3\right] - \alpha^2 \left[\frac{N_2}{N_1} q_{11} - \frac{N_6}{N_1} p_{11}\right] - c\,\frac{N_7 N_6}{N_1}(\dot{q}_{21} - \dot{q}_{11}) + k_1 \frac{N_6 N_8}{N_1}(q_{21} - q_{11}) \\ &+ k_\theta \frac{N_6 N_9}{N_1}(q_{21} - q_{11}) - k_3 \frac{N_7^2 N_9 N_6}{N_1}(q_{21} - q_{11})^3 + c_d q_{11} - b_0 \frac{N_6}{N_1}\cos(\Omega t) = 0 \end{aligned} \tag{38}$$

$$\ddot{p}_{11} - \beta^2 \frac{N_{11}}{N_{10}} p_{11} + \eta^2 \left[\frac{N_{12}}{N_{10}} q_{11} - p_{11}\right] + c_r \dot{p}_{11} = 0 \tag{39}$$

$$\ddot{r}_{21} - \beta^2 \left[\frac{N_{14}}{N_{13}} r_{21} + \frac{N_{15}}{N_{13}} {q_{21}}^2\right] + c_d \dot{r}_{21} = 0 \tag{40}$$

$$\begin{aligned} &\left(1 + \frac{M}{\rho A}\right)\ddot{q}_{21} - \beta^2 \left[2\frac{N_{15}}{N_{13}} r_{21} q_{21} + \frac{3}{2}\frac{N_{16}}{N_{13}} {q_{21}}^3\right] - \alpha^2 \left[\frac{N_{14}}{N_{13}} q_{21} - \frac{N_{17}}{N_{13}} p_{21}\right] + c\,\frac{N_7 N_{18}}{N_{13}}(\dot{q}_{21} - \dot{q}_{11}) \\ &- k_1 \frac{N_{18} N_8}{N_{13}}(q_{21} - q_{11}) - k_\theta \frac{N_{18} N_9}{N_{13}}(q_{21} - q_{11}) + k_3 \frac{{N_2}^2 N_9 N_{18}}{N_1}(q_{21} - q_{11})^3 + c_d \dot{q}_{11} = 0 \end{aligned} \tag{41}$$

$$\ddot{p}_{21} - \beta^2 \frac{N_{20}}{N_{19}} p_{21} + \eta^2 \left[\frac{N_{21}}{N_{19}} q_{21} - p_{21}\right] + c_r \dot{p}_{21} = 0 \tag{42}$$

where N_i coefficients are presented in the Appendix.

5 NUMERICAL RESULTS AND DISCUSSION

The numerical results are presented in this section. The mechanical properties of the case study are adopted from [4], and are listed in Table 1.

At first, the nonlinear behavior of the system in the presence of the nonlocal nonlinearity (large amplitude vibration of the substructures assumption) and absence of the local nonlinearity was examined. Which it means the nonlinear spring in the interface modelling was neglected. In order to obtain the frequency response of the system, the variable excitation frequency was chosen as a parameter which is varies around the natural frequency of the system, for which the first natural frequency of the system can be obtained by linearizing the equations of motion and can be expressed as $\omega_n = \lambda_n^2 \sqrt{EI/\rho A L^4}$, where λ is eigenvalues of the cantilever beam, and can be obtained from Eq. (33), and the other utilized parameters which are expressed in Table 1. Numerical simulations have been carried out for nonlinear system, Eqs. (34)-(39), by varying dimensionless excitation frequency Ω, the other non-dimensionalzed parameters which are assumed to be equal to $\beta = 138.564, \alpha = 103.395, \eta = 1.43\times10^4$, $b_0 = 0.001$, $c_d = 0.0035$ and $c_r = 0.0234$. The frequency responses of the first generalized coordinate of the transverse and rotation motions, are illustrated in Fig. 2, which shows the stable solutions of the nonlinear structure. It is seen that frequency curves are titled to the right which means system displays a hardening type for transverse motion and rotation. Depending on the initial values and excitation frequency, there might be two stable solutions or one stable solution in the frequency response of the system. Due to the existence of the stable and unstable points, there are two limit point bifurcations in the system, which the first one is responsible for a downward jump from a high amplitude motion to the low amplitude one, and the second one for a reverse scenario. Where the first and second bifurcation points correspond to $\Omega = 1.653$ (point A), and $\Omega = 1.694$ (point B), respectively. As shown in Fig. 2(a), when the nonlinear parameter starts from $\Omega = 1$ and continuously is increasing, the amplitude of the stable response gradually increased with increasing dimensionless excitation frequency until is reached to point A; as Ω is increased further a sudden jump occurs in the system, and takes place from point A to lower stable branch, point B, and if the excitation frequency is increased further the system continues stable branch by decreasing the stable amplitude of response.

Table 1
Physical properties of the bolted lap joint structure [4].

Symbol	Value	Unit	Description
L_b	260	*mm*	Length of the beams
L_t	500	*mm*	Total length of the system
t_b	5	*mm*	Thickness of the beams
M_t	0.1888	*kg*	Tip mass
h_1	30	*mm*	Length of the tip mass
h_2	32	*mm*	width of the tip mass
k_{aL}	8.089×10^8	*N/m*	Linear translational spring
$k_{\theta L}$	3264	*N/rad*	Linear torsional spring
$k_{\theta NL}$	3.722×10^8	N/m^3	Cubic torsional spring
c	0.281	*N.s/m*	Linear torsional damper
S	250	*mm*	Location of the bolted joint

Fig. 3 depicts the influence of the dimensionless parameter β on the frequency-response curves of the first generalized coordinate for the transverse and rotation motions, for the conditions and values of the Fig. 2. In addition, the different values of the β which are denoted on the figure, and the value of the α is selected as $\alpha = 0.75\beta$ due to the relation $\alpha = \sqrt{5/(7+6\upsilon)}\beta$. As shown in the Fig. 3, the dimensionless parameter β significantly affects the nonlinear resonance frequency and hysteresis region. It is seen that increasing β results in shift the nonlinear resonance frequency to higher excitation frequencies, and results decreasing in the maximum amplitude of the beam displacement. For instance, while $\beta = 138.564$, and for the transverse motion, the nonlinear resonance frequency occur at $\Omega = 1.649$, and by increasing the value of the β to values of 152.4204, 166.2768, it is observed that the corresponding nonlinear resonance frequencies altered to the values of $\Omega = 1.792,\ 1.935$, respectively.

Fig. 4 illustrates the influence of the dimensionless parameter η on the frequency-response curves of the first generalized coordinate for the transverse and rotation motions, for the conditions and values of the Fig. 2, and the different values of η which are denoted on the figure. It is seen that, the dimensionless parameter η significantly affects the nonlinear resonance frequency and hysteresis region, and the resonance region for the system gradually shifts from the right to the left as the η increases. Due to the fact that two limit point bifurcations get away from each other, hence, the entire region of the response becomes wider, which it results in increasing the maximum amplitude of the oscillation, and the corresponding nonlinear resonance frequency occurs at low excitation frequencies.

Fig. 5 shows the effect of the different values of the dimensionless base acceleration on the frequency-response curves of the system, for the values and conditions of the Fig. 2, and the dimensionless parameter η is assumed to be $\eta = 1.859\times10^{4}$. As it can be seen, as the forcing amplitude increases the maximum amplitude values of the oscillations increased, the frequency bandwidth of the system becomes wider.

Fig. 6 depicts the influence of the axial linear spring coefficient on the first generalized coordinate for the transverse and rotation motions for the conditions and values of the Fig. 2, and for different values of the linear spring constant which are denoted on the curves. It is seen that as the linear spring constant value increased the resonance frequency of the system increased and the maximum values of the transverse and rotation motions values are decreased. For instance, when the linear spring constant is assumed to be equal to $k_{aL} = 0.4$ *MN/m*, the resonance frequency and maximum amplitude are equal to 1.245 and 3.84×10^{-5}, respectively. As the linear spring stiffness is increased to the values of 0.7 *MN/m* and 1 *MN/m* the corresponding resonance frequencies are altered and occur at 1.306 and 1.367, respectively, and also the corresponding maximum amplitudes are changed to the values of 3.641×10^{-5} and 3.42×10^{-5}.

Fig. 7 depicts the effect of the nonlinear spring stiffness constant in the joint modelling on the first generalized coordinate for the transverse and rotation motions for the conditions and values of the Fig. 2, and for different values of the nonlinear spring constant which are denoted on the curves. It is seen that as the nonlinear spring constant increased, it resulted in strong hardening behavior in the system. For instance, while the nonlinear spring stiffness is equal to $k_{\theta NL} = 1$ *GN/m*^{3} the resonance frequency and maximum amplitude are equal to 1.229 and 6.508×10^{-5}, respectively. As the linear spring stiffness is increased to the values of 1.4 *GN/m*^{3} and 2 *GN/m*^{3} the corresponding resonance frequencies are altered and occur at 1.240 and 1.249, respectively, and also the corresponding maximum amplitudes are changed to the values of 4.997×10^{-5} and 4.089×10^{-5}.

Fig. 8 illustrates the effect of the different engineering beam theories namely, Timoshenko, Rayleigh and Euler-Bernoulli beam theories on the frequency response curves of the transverse motion for the values of the Fig. 2, and for the linear and nonlinear spring constants of the $k_{aL} = 0.4$ *MN/m* and $k_{\theta NL} = 2$ *GN/m*^{3}, respectively. It is seen that the system for different engineering beam theories has similar behavior but different maximum amplitudes and resonance frequencies. For example, for Timoshenko, Rayleigh and Euler-Bernoulli beam theories are occur at $\Omega = 1.424$, 1.83 and 2.234, respectively, and the corresponding maximum amplitudes are equal to 3.509×10^{-5}, 3.7×10^{-5} and 3.9×10^{-5}, respectively.

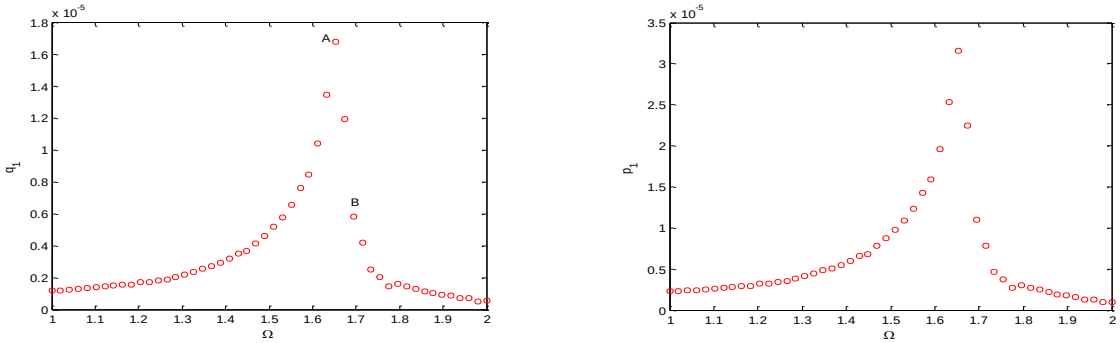

Fig.2
Frequency response of the system (a) The first generalized coordinate for the transverse motion (b) The first generalized coordinate for the rotation motion.

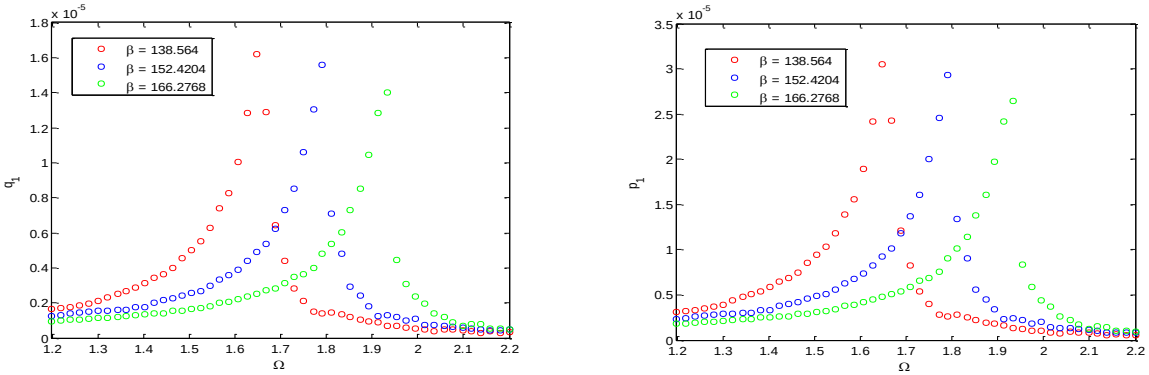

Fig.3
Influence of the dimensionless parameter β on the frequency response curves of the system (a) The first generalized coordinate for the transverse motion (b) The first generalized coordinate for the rotation motion.

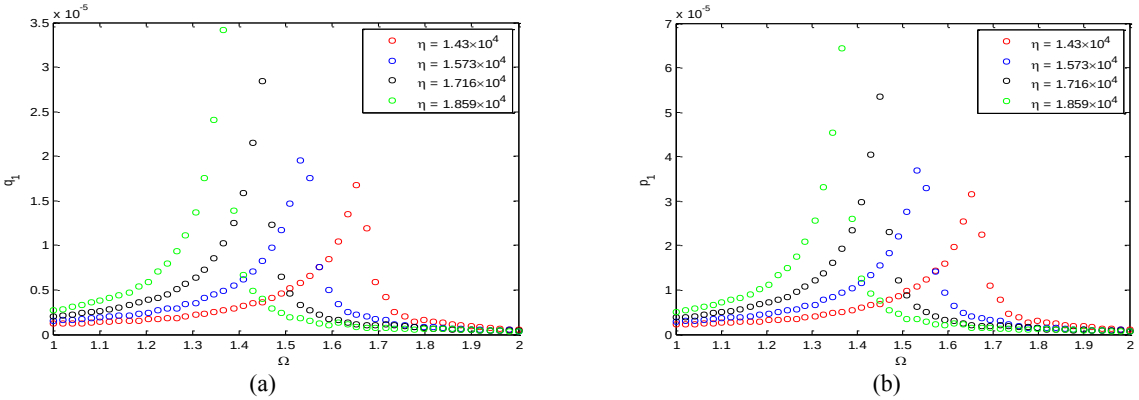

Fig.4
Influence of the dimensionless parameter η on the frequency response curves of the system (a) The first generalized coordinate for the transverse motion (b) The first generalized coordinate for the rotation motion.

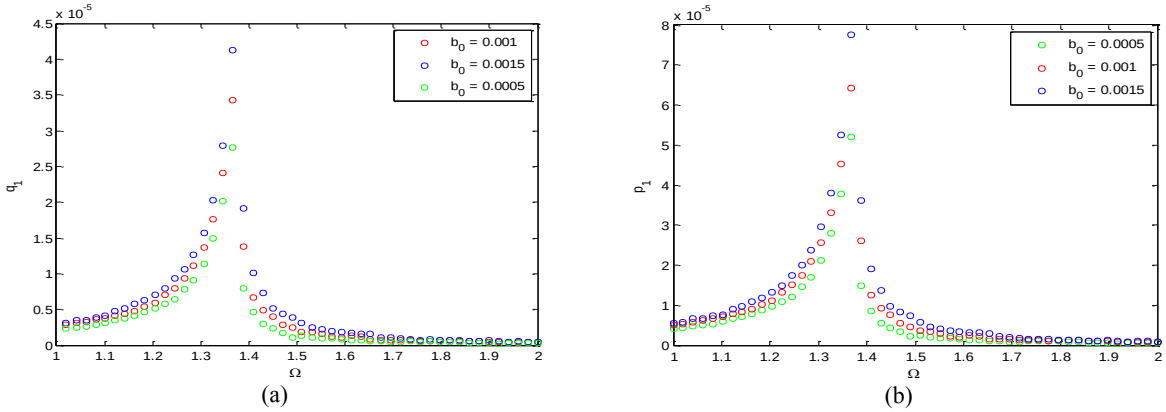

Fig.5
Effect of b_0 on the frequency response curves of the system (a) The first generalized coordinate for the transverse motion (b) The first generalized coordinate for the rotation motion.

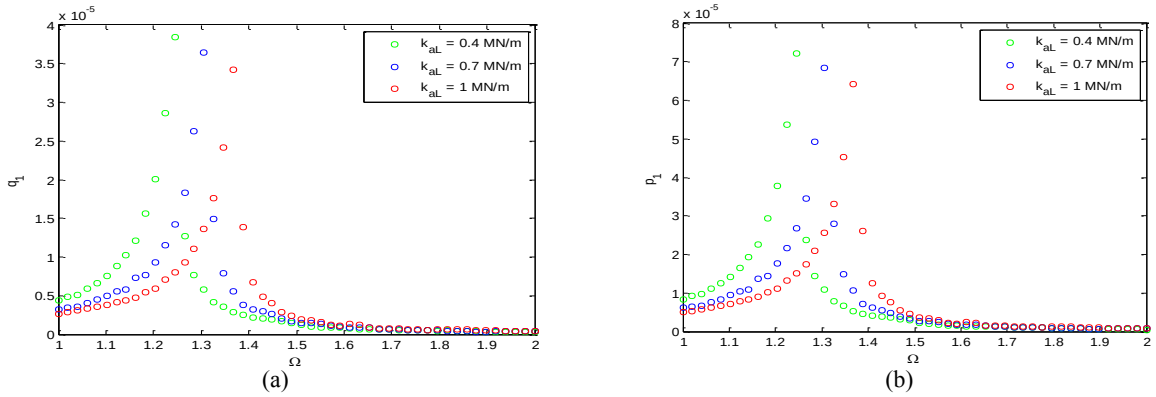

Fig.6
Effect of k_{aL} on the frequency response curves of the system (a) The first generalized coordinate for the transverse motion (b) The first generalized coordinate for the rotation motion.

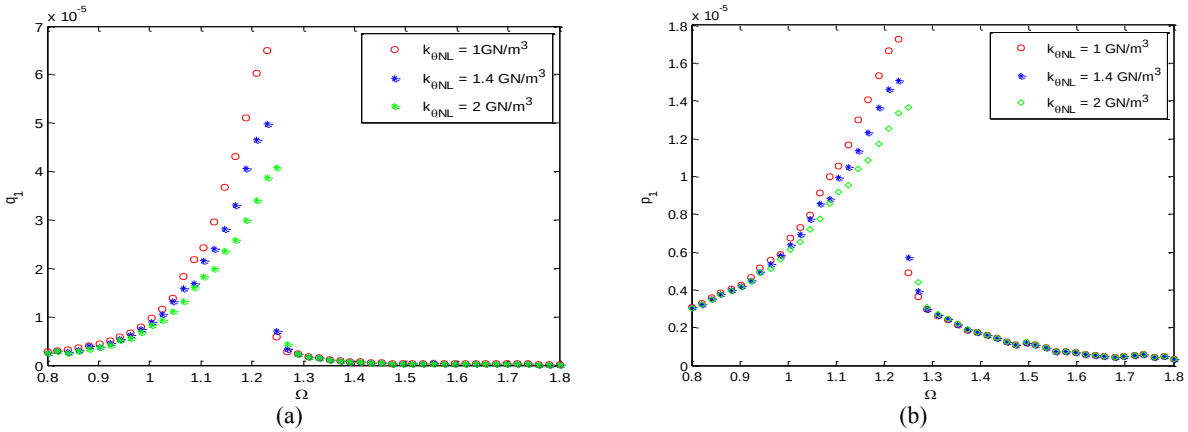

Fig.7
Effect of $k_{\theta NL}$ on the frequency response curves of the system (a) The first generalized coordinate for the transverse motion (b) The first generalized coordinate for the rotation motion.

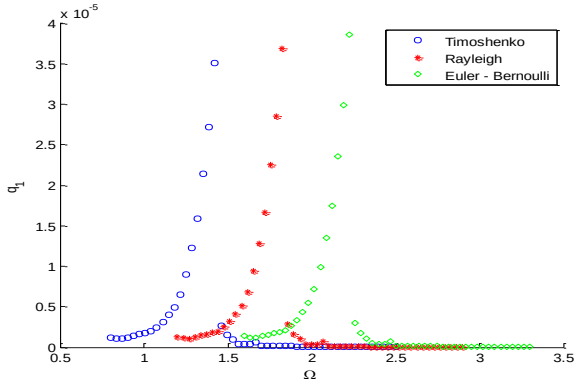

Fig.8
Effect of the different engineering beam theories on the frequency response curves of the system for the first generalized coordinate of the transverse motion.

6 CONCLUSIONS

In this paper a model for a Timoshenko beam by considering large amplitude vibration with a nonlinear bolted lap joint was presented. The joint was modelled using a combination of linear and nonlinear springs and linear torsional damper in order to model the softening phenomenon and energy dissipation of the joint interface due to the slip. The

governing equations of motion were derived using the Hamilton's principle. The reduced-order model equations were obtained based on Galerkin method. The set of coupled nonlinear equations were then solved using numerical simulation. A parametric study was carried out to reveal the influence of the different parameters such as, linear and nonlinear torsional spring, linear translational spring, and linear torsional damper on the vibration and stability of the bolted lap joint structure. The nonlinear behavior of the structure was examined in the absence of the nonlinear spring in the modelling of bolted lap joint. It was shown that the system in this case exhibit a hardening nonlinear behavior type due to the large amplitude vibration consideration in the substructures. Then, for the same system, the effect of the different dimensionless parameters on the frequency-response curves and hysteresis region of the system were investigated. It was shown that the dimensionless parameter β significantly affects the frequency-response curves, in which as the value of the β increased, resulted in increasing the resonance frequency and decreasing in maximum amplitudes of the system. Moreover, the influence of the dimensionless parameter η on the frequency-response curves was studied. It was illustrated that η remarkably affect both natural and resonance frequencies, and as η increased it resulted in shifting the natural and resonance frequencies to the left. Furthermore, the effect of the forcing amplitude was investigated. It was shown that the forcing amplitude effect on the hardening behavior of the system and as the forcing amplitude increased it resulted in widening the frequency response amplitude. Then, the effect of the presence of the linear and nonlinear springs in the joint modelling was studied. At first, the effect of the linear spring, in the absence of the nonlinear spring, on the frequency-response curves was investigated. It was shown that presence of the linear spring increases both natural and resonance frequencies and decreases the maximum amplitudes of the system. In addition, the effect of the nonlinear spring, in the absence of the linear spring, on the frequency-response curves was demonstrated. It was shown that presence and increasing the nonlinear spring stiffness coefficient value results in strong hardening-type behavior and decreasing the maximum amplitude compared to the absence of the linear and nonlinear springs. Furthermore, the effect of the different engineering beam theories on the system response was studied. It was shown that Euler-Bernoulli beam theory by neglecting the effects of the shear deformations and rotary inertia over-predicts the natural frequency.

APPENDIX

$$N_1=\int_0^1 \varphi_1^{\,2}\,dx,\quad N_2=\int_0^1 \varphi_1\varphi_1''\,dx,\quad N_3=\int_0^1 \varphi_1\varphi_1'\varphi_1''\,dx,\quad N_4=\int_0^1 \varphi_1\varphi_1'^{2}\varphi_1''\,dx,$$

$$N_5=\int_0^1 \varphi_1\psi_1'\,dx,\quad N_6=\int_0^1 \varphi_1 dx,\quad N_7=\varphi_1'(S),\quad N_8=\varphi_1(S),$$

$$N_9=\varphi_1''(S),\quad N_{10}=\int_0^1 \psi_1^{\,2}dx,\quad N_{11}=\int_0^1 \psi_1\psi_1''\,dx,\quad N_{12}=\int_0^1 \psi_1\varphi_1'\,dx,$$

$$N_{13}=\int_1^2 \varphi_1^{\,2}dx,\quad N_{14}=\int_1^2 \varphi_1\varphi_1''\,dx,\quad N_{15}=\int_1^2 \varphi_1\varphi_1'\varphi_1''\,dx,\quad N_{16}=\int_1^2 \varphi_1\varphi_1'^{2}\varphi_1''\,dx,$$

$$N_{17}=\int_1^2 \varphi_1\psi_1'\,dx,\quad N_{18}=\int_1^2 \varphi_1 dx,\quad N_{19}=\int_1^2 \psi_1^{\,2}dx,\quad N_{20}=\int_1^2 \psi_1\psi_1''\,dx,$$

$$N_{21}=\int_1^2 \psi_1\varphi_1'\,dx,\quad A_1=\varphi_1(L_t),\quad A_2=\varphi_1'(L_t)$$

REFERENCES

[1] Lee U., 2001, Dynamic characterization of the joints in a beam structure by using spectral element method, *Shock and Vibration* **8**: 357-366.

[2] Haines R., 1980, Survey: 2-dimensional motion and impact at revolute joints, *Mechanism and Machine Theory* **15**: 361-370.

[3] Flores P., Ambrósio J., 2004, Revolute joints with clearance in multibody systems, *Computers & Structures* **82**: 1359-1369.

[4] Ahmadian H., Jalali H., 2007, Identification of bolted lap joints parameters in assembled structures, *Mechanical Systems and Signal Processing* **21**: 1041-1050.

[5] Ma X., Bergman L., Vakakis A., 2001, Identification of bolted joints through laser vibrometry, *Journal of Sound and Vibration* **246**: 441-460.

[6] Jalali H., Ahmadian H., Mottershead J.E., 2007, Identification of nonlinear bolted lap-joint parameters by force-state mapping, *International Journal of Solids and Structures* **44**: 8087-8105.

[7] Liao X., Zhang J., 2016, Energy balancing method to identify nonlinear damping of bolted-joint interface, *Key Engineering Materials* **693**: 318-323.

[8] Chatterjee A., Vyas N.S., 2003, Non-linear parameter estimation with Volterra series using the method of recursive iteration through harmonic probing, *Journal of Sound and Vibration* **268**: 657-678.
[9] Chatterjee A., Vyas N.S., 2004, Non-linear parameter estimation in multi-degree-of-freedom systems using multi-input Volterra series, *Mechanical Systems and Signal Processing* **18**: 457-489.
[10] Kerschen G., Worden K., Vakakis A.F., Golinval J.-C., 2007, Nonlinear system identification in structural dynamics: current status and future directions, *In 25th International Modal Analysis Conference*, Orlando.
[11] Thothadri M., Moon F., 2005, Nonlinear system identification of systems with periodic limit-cycle response, *Nonlinear Dynamics* **39**: 63-77.
[12] Thothadri M., Casas R.A., Moon F.C., D'Andrea R., Johnson Jr C.R., 2003, Nonlinear system identification of multi-degree-of-freedom systems, *Nonlinear Dynamics* **32**: 307-322.
[13] Hajj M.R., Fung J., Nayfeh A.H., Fahey S.O'F., 2000, Damping identification using perturbation techniques and higher-order spectra, *Nonlinear Dynamics* **23**: 189-203.
[14] Noël J.P., Kerschen G., 2016, 10 years of advances in nonlinear system identification in structural dynamics: A review, *In Proceedings of ISMA 2016-International Conference on Noise and Vibration Engineering*.
[15] Di Maio D., 2016, Identification of dynamic nonlinearities of bolted structures using strain analysis, *Nonlinear Dynamics* **1**: 387-414.
[16] Ahmadian H., Azizi H., 2011, Stability analysis of a nonlinear jointed beam under distributed follower force, *Journal of Vibration and Control* **17**: 27-38.
[17] Cooper S., Di Maio D., Ewins D, 2017, Nonlinear vibration analysis of a complex aerospace structure, *Nonlinear Dynamics* **1**: 55-68.
[18] Jahani K., Nobari A., 2008, Identification of dynamic (Young's and shear) moduli of a structural adhesive using modal based direct model updating method, *Experimental Mechanics* **48**: 599-611.
[19] Li WL., 2002, A new method for structural model updating and joint stiffness identification, *Mechanical Systems and Signal Processing* **16**: 155-167.
[20] Ratcliffe M., Lieven N., 2000, A generic element-based method for joint identification, *Mechanical Systems and Signal Processing* **14**: 3-28.
[21] Wang J., Chuang S., 2004, Reducing errors in the identification of structural joint parameters using error functions, *Journal of Sound and Vibration* **273**: 295-316.
[22] Segalman D.J., Paez T., Smallwood D., Sumali A., Urbina A., 2003, *Status and Integrated Road-Map for Joints Modeling Research*, Sandia National Laboratories, Albuquerque.
[23] Shokrollahi S., Adel F., 2016, Finite element model updating of bolted lap joints implementing identification of joint affected region parameters, *Journal of Theoretical and Applied Vibration and Acoustics* **2**: 65-78.
[24] Ren Y., Beards C., 1998, Identification of'effective'linear joints using coupling and joint identification techniques, *Journal of Vibration and Acoustics* **120**: 331-338.
[25] Ghorbanpour Arani A., Atabakhshian V., Loghman A., Shajari A.R., Amir S., 2012, Nonlinear vibration of embedded SWBNNTs based on nonlocal Timoshenko beam theory using DQ method, *Physica B: Condensed Matter* **47**: 2549-2555.
[26] Ghorbanpour Arani A., Kolahchi R., 2014, Nonlinear vibration and instability of embedded double-walled carbon nanocones based on nonlocal Timoshenko beam theory, *Proceedings of the Institution of Mechanical Engineers, Part C: Journal of Mechanical Engineering Science* **228**: 690-702.
[27] Ghorbanpour Arani A., Dashti P., Amir S., Yousefi M., 2015, Nonlinear vibration of coupled nano- and microstructures conveying fluid based on Timoshenko beam model under two-dimensional magnetic field, *Acta Mechanica* **226**: 2729-2760.
[28] Rao S.S., 2007, *Vibration of Continuous Systems*, John Wiley & Sons.
[29] Stanton S.C., Erturk A., Mann B.P., Inman D.J., Inman D.J., 2012, Nonlinear nonconservative behavior and modeling of piezoelectric energy harvesters including proof mass effects, *Journal of Intelligent Material Systems and Structures* **23**: 183-199.
[30] Firoozy P., Khadem S.E., Pourkiaee S.M., 2017, Broadband energy harvesting using nonlinear vibrations of a magnetopiezoelastic cantilever beam, *International Journal of Engineering Science* **111**: 113-133.
[31] Ghayesh M.H., Amabili M., Farokhi H., 2013, Three-dimensional nonlinear size-dependent behaviour of Timoshenko microbeams, *International Journal of Engineering Science* **71**: 1-14.
[32] Reddy J.N., 2004, *Mechanics of Laminated Composite Plates and Shells: Theory and Analysis*, CRC press.
[33] Firoozy P., Khadem S.E., Pourkiaee S.M., 2017, Power enhancement of broadband piezoelectric energy harvesting using a proof mass and nonlinearities in curvature and inertia, *International Journal of Mechanical Sciences* **133**: 227-239.
[34] Pourkiaee S.M., Khadem S.E., Shahgholi M., 2016, Parametric resonances of an electrically actuated piezoelectric nanobeam resonator considering surface effects and intermolecular interactions, *Nonlinear Dynamics* **84**: 1943-1960.
[35] Han S.M., Benaroya H., Wei T., 1999, Dynamics of transversely vibrating beams using four engineering theories, *Journal of Sound and Vibration* **225**: 935-988.